Vailable online at www.sciencedirect.com

SciVerse ScienceDirect

Energy Procedia 27 (2012) 355 – 360

Energy Procedia

SiliconPV: April 03-05, 2012, Leuven, Belgium

Al_2O_3 surface passivation characterized on hydrophobic and hydrophilic *c*-Si by a combination of QSSPC, CV, XPS and FTIR

H. Goverde[a,b], B. Vermang[a,c], A. Morato[a,d], J. John[a], J. Horzel[a], G. Meneghesso[d], J. Poortmans[a,c]

[a]*IMEC, Kapeldreef 75, 3001 Heverlee, Belgium*
[b]*Eindhoven University of Technology (TU/e), P.O. Box 513, 5600 MB Eindhoven, The Netherlands*
[c]*Katholieke Universiteit Leuven (ESAT), Kasteelpark Arenberg 10, 3001 Heverlee, Belgium*
[d]*Dept. of Information Engineering University of Padova, Via Gradenigo 6B, 35131 Padova, Italy*

Abstract

In this work, the influence of the *c*-Si surface finishing (hydrophobic/hydrophilic) prior to the deposition of the Al_2O_3 passivation layer on the passivation quality is investigated. The samples are characterized by a combination of Quasi-Steady-State-PhotoConductance (QSSPC) Capacity-Conductance (CV), X-ray Photoelectron Spectroscopy (XPS) and Fourier Transformed InfraRed (FTIR) measurements. Furthermore, FTIR measurements are used to determine the thickness of interfacial SiO_x layer.

Keywords: Si; Surface Passivavation; Al_2O_3; FTIR; CV; XPS; QSSPC

1. Introduction

Thin (<30 nm) Al_2O_3 layers has been proven to provide an excellent level of surface passivation of *n*- and *p*-type *c*-Si due to its unique property of a high negative fixed charge density (Q_f) and a low interface defect density (D_{it}) [1]. In the field-effective passivation mechanism, interfacial SiO_x layers between the bulk Al_2O_3 and the *c*-Si play an important role [2-4]. The thickness and the quality of the SiO_x interfacial layer is influenced by the *c*-Si surface state prior to deposition and the post-deposition anneal [1-6].

In this work, Al_2O_3 films were deposited on *c*-Si with oxidized or H-terminated surfaces. Prior and after post-deposition anneal, effective minority carrier lifetimes were measured using QSSPC. For Al_2O_3 layers on Czochralski (CZ) grown silicon, the fixed charge density and the interface defect density were determined using Capacitance-Voltage (C-V) measurements. Al_2O_3/SiO_x structures layers were characterized using non-destructive Fourier Transform Infrared Spectroscopy (FTIR) and X-ray

doi:10.1016/j.egypro.2012.07.076

Photoelectron Spectroscopy (XPS). Furthermore, it will be shown that the thickness of the interfacial SiO_x layer can be calculated using non-destructive FTIR measurements.

2. Experimental

Al_2O_3 layers (30 nm) were deposited using thermal Atomic Layer Deposition (ALD) ($Al(CH_3)_3$ + H_2O) at a temperature (T_{dep}) of 200 ˚C, on both sides of 4" mirror polished *p*-type Float-Zone (FZ) *c*-Si with a resistivity of 2 Ω·cm and a thickness of 200 µm. Table 1 shows the cleaning process prior to Al_2O_3 deposition by ALD.

Table 1. Schematic overview of *c*-Si cleaning process to achieve the hydrophobic (left) or hydrophilic (right) *c*-Si surface state

Hydrophobic

	Solution	*Time*
1	H_2O + HF (2%) + HCl (5%)	5 min.

Hydrophilic

	Solution	*Time*
1.	H_2O + HF (2%) + HCl (5%)	5 min.
2.	$NH_4OH + H_2O_2 + H_2O$ (1:1:5)	10 min.

The samples received a post-deposition thermal anneal in N_2 environment for 20 min. at a temperature of 300, 500 or 800 ˚C. FTIR spectra were constructed from 400 to 4000 cm^{-1} by a Brucker TENSOR FT-IR spectrometer. Furthermore, the effective carrier lifetimes in the *c*-Si sample (τ_{eff}) were measured by QSSPC measurement using a Sinton instrument lifetime tester in the generalized mode at an injection level of $\Delta n = 1\times10^{14}$ (low) or at $\Delta n = 1\times10^{15}$ (high) cm^{-3}. Prior and after post-deposition anneal (20 min. 300 ˚C), the thickness of the interfacial SiO_x layer between a 3 nm thick Al_2O_3 layer and the *c*-Si surface was measured using a Thermo Fish Theta 300 XPS spectrometer at an analyzing angle of 28˚.

Furthermore, Al_2O_3 films with a thickness of 5, 10, 15 or 20 nm were synthesized by an equivalent deposition process as described above, on both sides of 4" Saw Damage Removed (SDR) *p*-type Czochralski (CZ) *c*-Si with a resistivity of 1.5 Ω·cm and a thickness of 150 ± 10 µm with hydrophilic or hydrophobic surfaces. The Al_2O_3 layers were removed from the rear by HF vapor, prior to the deposition of 2 µm thick Al layer by e-beam evaporation. Pt dots electrodes with an area of $(2.0 \pm 0.5) \times 10^{-3}$ cm^2 were sputtered on the front, after the activation of the passivation layer by a thermal anneal as described above. Capacity-Voltage and Conductance-Voltage measurements were recorded using HP 4156 precision LCR-meter at low and high (1 – 100 kHz) frequency. All measurements were carried out at room temperature.

30 nm thick Al_2O_3 films were grown using the thermal ALD process as above, on both sides of 4" mirror polished *p*-type FZ *c*-Si with a resistivity of 2 Ω·cm and a thickness of 200 µm capped by a thermal grown SiO_x layer with varying layer thickness. The SiO_x layer thickness is varied by etching 100 nm thick, high quality, thermal grown (1050 ˚C) SiO_x layers using a buffer HF solution. The thickness was determined by Spectroscopic Ellipsometry (SE) (SENTECH SE400adv-PV) prior to Al_2O_3 deposition. FTIR spectra from 400 to 4000 cm^{-1} were constructed by a Brucker TENSOR FT-IR spectrometer.

3. Result/Discussion

3.1. c-Si surface finishing

Effective minority carrier lifetimes ($\Delta n = 1\times10^{15}$ cm^{-3}) in H-terminated and oxidized *c*-Si samples passivated by Al_2O_3 are shown in Fig. 1(a) as a function of the post-deposition annealing temperature. Furthermore, the ratio between τ_{eff} at low ($\Delta n = 1\times10^{14}$ cm^{-3}) injection level and high ($\Delta n = 1\times10^{15}$ cm^{-3}) injection level is calculated, see Fig. 1(b).

Fig. 2(a) displays the fixed charge density and the interface defect density of *c*-Si samples passivated by an Al_2O_3 layer with a thickness of 10 nm as a function of the annealing temperature. Fig. 2(b) shows the thickness of the Al_2O_3 and interfacial SiO_x layers prior and after a thermal anneal at 300 ˚C.

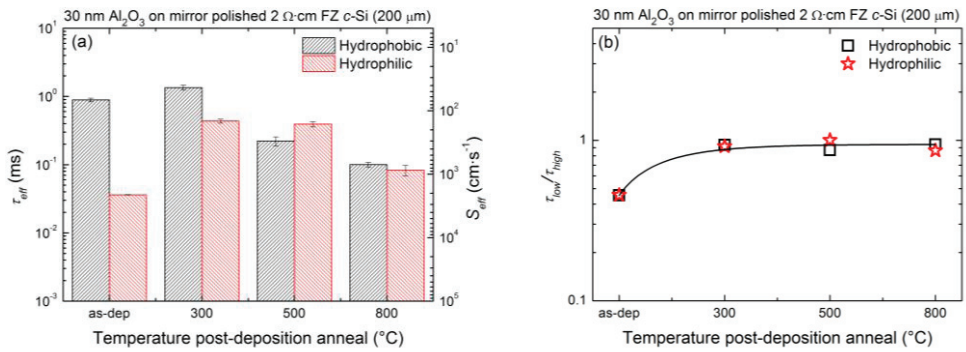

Fig. 1. Passivation properties of ALD Al_2O_3 deposited on *c*-Si with H-terminated or oxidized surface after an anneal at a temperature displayed on the x-axis (N_2, 20 min.) (a) Effective carrier lifetime at $\Delta n = 1\times10^{15}$ cm^{-3} (b) ratio between effective carrier lifetime at low ($\Delta n = 1\times10^{14}$ cm^{-3}) injection level and high ($\Delta n = 1\times10^{15}$ cm^{-3}) injection level. The black line is a guide for the eye

The Al_2O_3 layer and the Si/Al_2O_3 interface is furthermore characterized using FTIR. The absorption and differential spectrum of as-deposited Al_2O_3 layers is shown in Fig. 3(a) and Fig. 3(b) displays the absorption and differential spectrum of Al_2O_3 after a post-deposition anneal at 800 °C.

3.2. As-deposited

For as-deposited layers, lower surface recombination velocities are observed for Al_2O_3 deposited on *c*-Si with H-terminated surface. This difference is caused by a higher interface defect density for Al_2O_3 deposited on *c*-Si with an oxidized surface, as shown in Fig. 2(a). Fig. 2(b) shows the presence of 1.0 nm thick interfacial SiO_x layer, grown by the wet-chemical oxidation step. The low-quality oxide layer on the *c*-Si surfaces provides a poor chemical passivation, resulting in surface recombination velocity of 270 ± 20 cm·s^{-1}. A surface recombination velocity of 11 ± 2 cm·s^{-1} has been observed in *c*-Si samples with hydrophobic surface prior Al_2O_3 deposition due to the low D_{it}.

A positive fixed charge density (Q_f = (8 ± 2) ×10^{11} cm^{-2}) is reported for as-deposited layers. The presence of positive charges is also indicated by the low τ_{low}/τ_{high} ratio. Martin *et al.* hypothesized that an inversion layer in the subsurface region, present due to the absence of negative fixed charges, is responsible for the reduction of lifetime at low injection level [7].

Absorption peaks related to Al-O and O-H bonds are present in the FTIR spectrum. In contrast with Al_2O_3 layers synthesized by plasma-assisted ALD using $Al(CH_3)_3$ and an O_2 plasma, no C-H absorption peak is observed in the noise signal [1,8]. The H_2O precursor is less volatile than O radicals from the oxygen plasma; therefore, less C contamination is incorporated. The differential spectrum demonstrates by an absorption peak (1060 cm^{-1}) which originates from the TO mode of thermally grown amorphous SiO_x the difference between both Al_2O_3/Si interfaces [9]. The absorption peak indicates the presence of a interfacial SiO_x layer between the Al_2O_3 layer and the *c*-Si with hydrophilic surface finishing. No significant difference is visible for the absorption peak associated with Si-H bonds.

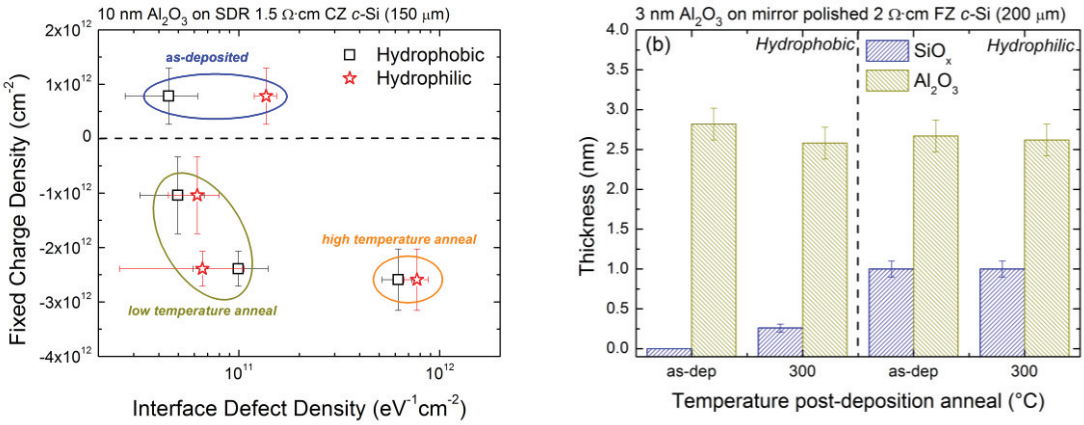

Fig. 2. (a) Q_f and D_{it} of 10 nm as-deposited, low (≤ 500 ˚C) or high (> 500 ˚C) temperature annealed Al_2O_3 deposited on the hydrophilic or hydrophobic *c*-Si surface states. (b) Al_2O_3 and SiO_x thickness of as-deposited and annealed (N_2, 20 min. at 300 ˚C) *c*-Si samples with hydrophilic or hydrophobic surface

3.3. Post-deposition anneal

An excellent level of passivation is reported for both surface finishing after a post-deposition anneal at T_{ann} = 300 ˚C; S_{eff} decreases to 7.5 ± 0.5 cm·s^{-1} and 22 ± 2 cm·s^{-1} for Al_2O_3 deposited on *c*-Si in the hydrophobic or hydrophilic surface state respectively. Fixed negative charges are formed in the passivation layer (Q_f = - (1.0 ± 0.7) ×10^{12} cm^{-2} for T_{ann} = 300 ˚C) and the interface defect density of *c*-Si samples with a hydrophilic surface state decreases while the D_{it} of passivated *c*-Si samples with hydrophobic surface finishing prior to Al_2O_3 deposition remained low (D_{it} = (5 ±1) ×10^{10} and (6 ± 1) ×10^{10} cm^{-2} for hydrophobic and hydrophilic surface finishing respectively after a thermal anneal at T_{ann} = 300 ˚C). Also the ratio τ_{low}/τ_{high} of both surface finishes indicates that no subsurface inversion layer is present after anneal due to the fixed negative charges in the passivation layer.

Fig 2(b) shows the formation of an interfacial SiO_x layer between the Al_2O_3 and the hydrophobic *c*-Si surfaces after a thermal anneal at 300 ˚C while the thickness of the SiO_x interfacial layer between Al_2O_3 and the hydrophilic *c*-Si surfaces remains constant. The formation of a high quality (confirmed by a low D_{it}) interfacial SiO_x layer for both *c*-Si surface finishes is also depicted by an absorption peak at 1060 cm^{-1} in the FTIR spectrum.

For T_{ann} = 500 ˚C, the fixed charge density (Q_f = - (2.4 ± 0.4) ×10^{12} cm^{-2}) increases compared with layers annealed at 300 ˚C, the interface defect density increases slightly (D_{it} = (10 ±1) ×10^{10} and (7 ± 1) ×10^{10} cm^{-2} for hydrophobic and hydrophilic surface finishing respectively, leading to an increase of the effective surface recombination velocity. No difference in surface passivation is observed between both surface finishes. By inspecting the differential spectrum, an interfacial SiO_x layer of equivalent thickness is confirmed by the absence of an absorption peak at 1060 cm^{-1}.

At T_{ann} > 500 ˚C, surface recombination velocities increase due to blistering formation and an increase of the interface defect density (see Fig. 2(a)) [10]. Si-H bonds break at higher annealing temperature and H is effused from the *c*-Si interface resulting in dangling bonds, and therefore, an increase of the D_{it} [11]. The use of forming gas (H_2) during the annealing would probably prevent the increase of D_{it}. Furthermore, fixed charges are removed from the *c*-Si surface due to blistering of the passivation layer. The negative fixed charge density is not affected by the high (> 500 ˚C) annealing temperature, leading to the conclusion that the level of passivation is reduced due to blistering formation and an increase of the interface defect density.

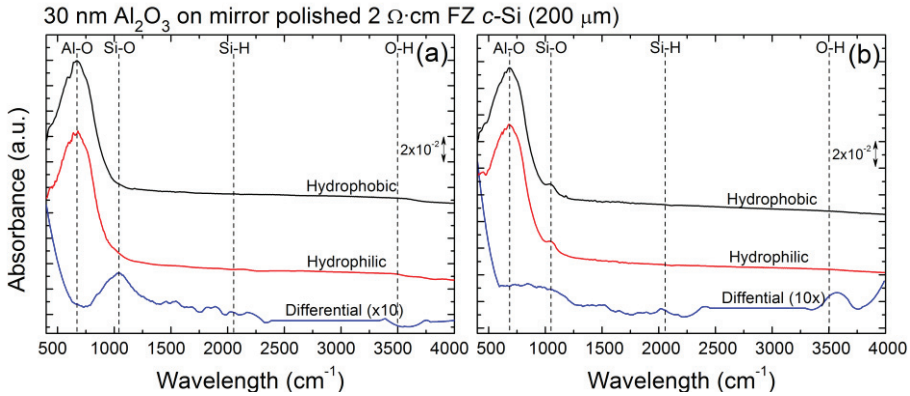

Fig. 3. Infrared absorption spectra of 30 nm Al_2O_3 deposited on both sides of *c*-Si with hydrophobic or hydrophilic surfaces. The differential absorption spectrum is displayed to indicate the difference between the passivation layers. (a) The spectrum of as-deposited Al_2O_3 layers and (b) after a post-deposition anneal (N_2, 20 min. at 500 ˚C). The spectra are off-set for clarity

3.4. Interfacial SiO_x thickness

As described in Section 3.1 above, the interfacial SiO_x layer causes an absorption peak at 1060 cm^{-1} in the FTIR spectrum. For non-destructive determination of the thickness of the interfacial SiO_x layer after annealing, FTIR spectra of $Al_2O_3/SiO_x/c$-Si structures with 30 nm thick Al_2O_3 and varying SiO_x thickness are constructed. Fig. 4 shows the absorbance at 1060 cm^{-1} as a function of the SiO_x thickness.

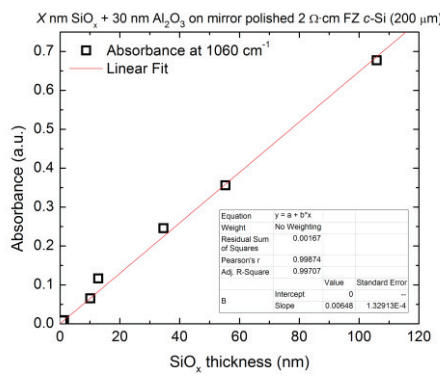

Fig. 4. Absorbance at 1060 cm^{-1} of the $Al_2O_3/SiO_x/c$-Si samples a function of the SiO_x thickness. The SiO_x thickness has been measured by SE prior to the deposition of the 30 nm thick Al_2O_3 layer by ALD

As displayed in Fig. 4, the absorbance at 1060 cm^{-1} depends linearly on the thickness of the SiO_x layer. This can be understood, since, FTIR spectra apply to Lambert-Beer's law:

$$-ln[I/I_0] = \alpha l \qquad (1)$$

With I the transmittance intensity of the sample, I_0 the absorbance of the reference sample (bare *c*-Si), the α absorbance coefficient and l the transmittance length. Eq. (1) shows that the logarithm of the absorption divided by the absorption of the reference sample depends linearly on the transmittance length. Therefore, Fig. 4 can be used to determine the thickness of the SiO_x layer after a thermal treatment, under the assumption that the quality of the SiO_x interlayer is equal to the quality of the thermally grown SiO_x layer. The linear fit shows that $\alpha = (6.5 \pm 0.1) \times 10^{-3}$ nm^{-1}, leading to a SiO_x thickness of 2.0 ± 0.2 and 1.7

± 0.2 nm for the hydrophilic and hydrophobic *c*-Si finishing respectively after a post-deposition anneal at 500 ˚C, thus, no difference interfacial SiO_x layer is observed between both *c*-Si surface finishes after a thermal anneal at 500 ˚C.

4. Conclusion

The influence of the *c*-Si surface finishing on the characteristics of Al_2O_3 passivation layers has been investigated by a combination of FTIR, CV, XPS and QSSPC measurements. It has been proven that FTIR is powerful, non-destructive technique to characterize the thickness of the interfacial SiO_x layer. The interface defect density is the dominating parameter for the surface passivation quality. The hydrophobic *c*-Si surface finishing is preferred because of the low D_{it} for as-deposited layers; however, an equivalent level of surface passivation has been observed after a thermal treatment. For both thicknesses, a high quality SiO_x interfacial layer is formed during a thermal treatment.

Acknowledgements

The authors greatly acknowledge the support of the IMEC Industrial Affiliated Partner (IIAP-PV) program and the IMEC PV support team. T. Bearda and S. Granada are kindly acknowledged for the FTIR measurements.

References

[1] Hoex B, Heil SBS, Langereis E, van de Sanden MCM, Kessels WMM, Ultralow surface recombination of *c*-Si substrates passivated by plasma-assisted atomic layer deposition Al_2O_3, *Appl Phys Lett,* 2006;**89**, 04112 .

[2] Agostinelli G, Delabie A, Vitanov P, Alexieva Z, Dekkers HFW, De Wolf S, Beaucarne G, Very low surface recombination velocities on p-type silicon wafers passivated with a dielectric with fixed negative charge, *Sol Energ Mater Sol C,* 2006; **90**, 3438-3443

[3] Werner F, Veith B, Zielke D, Kuhnemund L, Tegenkamp C, Electronic and chemical properties of the *c*-Si/Al_2O_3 interface, *J Appl Phys*, 2011; **109**, 113701

[4] Benick J, Richter A, Li TTA, Grant NE, Mcintosh KR, Ren Y, Weber KJ, Hermle M, Glunz SW, Effect of a post-deposition anneal on Al_2O_3 properties, 35th IEEE PVSC, Honolulu, 2010; **2**, 891-896

[5] Verlaan V. van den Elzen LRJG, Dingemans G, van de Sanden MCM, Kessels WMM, Composition and bonding structure of plasma-assisted ALD Al_2O_3 films, *Phys Status Solidi C 7*, 2010; **3-4** 976-979

[6] Dingemans G, Terlinden NM, Verheijen MA, van de Sanden MCM, Kessels WMM, Controlling the fixed charges and passivation properties of Si(100)/Al_2O_3 interfaces using ultrathin SiO_2 interlayers sythesized by atomic deposition, *J Appl Phys*, 2011; **110**, 093715

[7] Martin I, Hoex B, van de Sanden MCM, Alcubilla R, Kessels WMM, The origin of emitter-like recombination for inverted c-Si surfaces, *Proc 23rd European PVSEC*, Valencia, 2008; 1388

[8] Langereis E, Keijmel J, van de Sanden MCM, Kessels WMM, Surface chemistry of plasma-assisted atomic layer deposition of Al_2O_3 studied by infrared spectroscopy, *Appl Phys Lett*, 2008; **92**, 231904

[9] Kirk CT, Quantitative analysis of the effect of disorder-induced mode coupling on infrared absorption in silica, *Phys Rev B*, 1988; **38**, 1255-1273

[10] Vermang B, Goverde H, Uruena A, Lorenz A, Cornagliotti E, Rothschild A, John J, Poortmans J, Mertens R, Blistering in ALD Al_2O_3 passsivation layers as rear contacting for local Al BSF Si solar cells, *Sol Energ Mat Sol C,* in press

[11] Dingemans G, Engelhart P, Seguin R, Einsele F, Hoex B, van de Sanden MCM, Kessels WMM, Stability of Al_2O_3 and Al_2O_3/a-SiN_x:H stacks for surface passivation of crytalline silicon, *J Appl Phys*, 2009; **106**, 114907